
Figures and figure supplements

Characterization of TSET, an ancient and widespread membrane trafficking complex

Jennifer Hirst, et al.

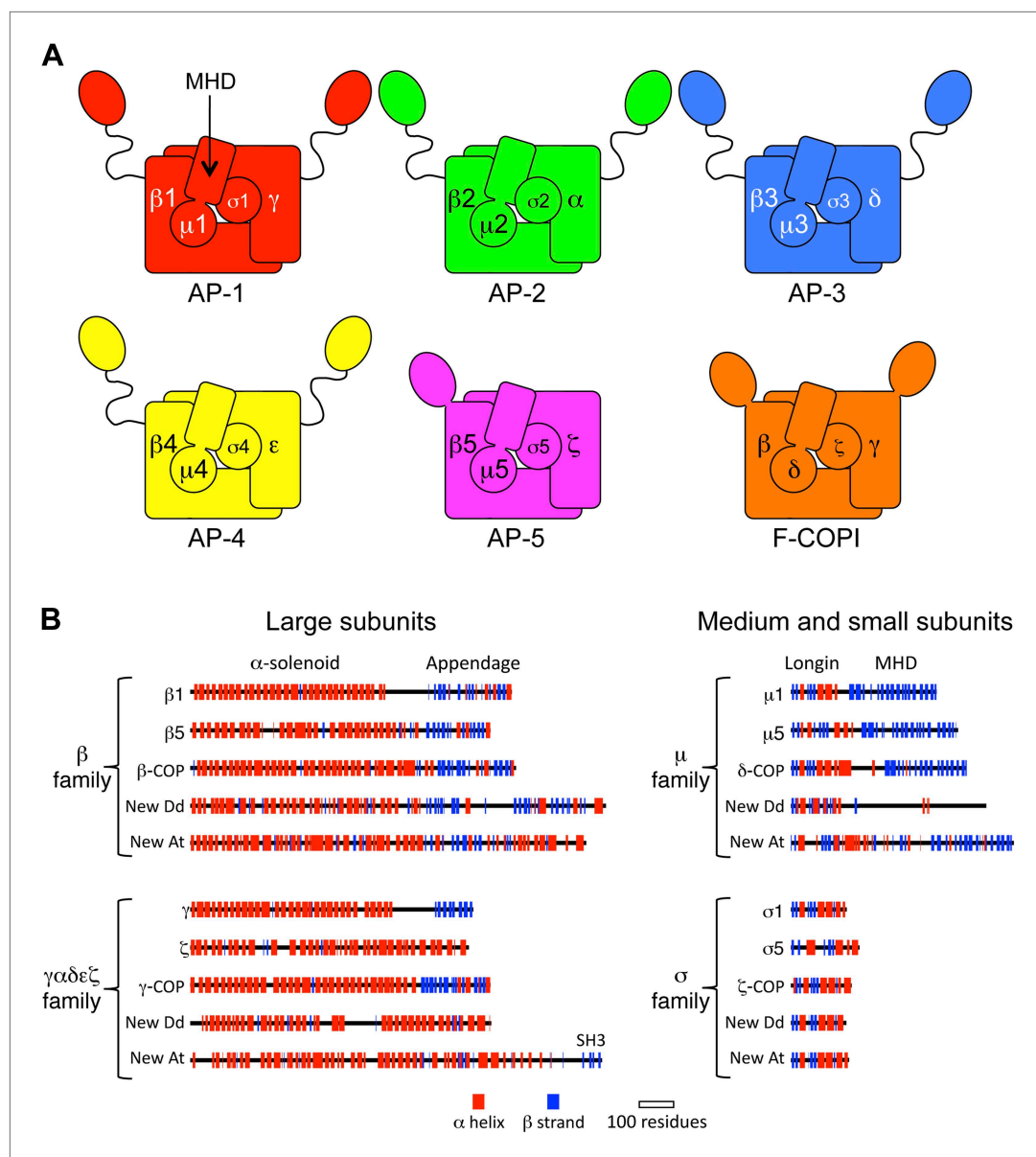


Figure 1. Diagrams of APs and F-COPI. **(A)** Structures of the assembled complexes. All six complexes are heterotetramers; the individual subunits are called adaptins in the APs (e.g., γ -adaptin) and COPs in COPI (e.g., γ -COP). The two large subunits in each complex are structurally similar to each other. They are arranged with their N-terminal domains in the core of the complex, and these domains are usually (but not always) followed by a flexible linker and an appendage domain. The medium subunits consist of an N-terminal longin-related domain followed by a C-terminal μ homology domain (MHD). The small subunits consist of a longin-related domain only. **(B)** Jpred secondary structure predictions of some of the known subunits (all from *Homo sapiens*), together with new family members from *Dictyostelium discoideum* (Dd) and *Arabidopsis thaliana* (At). See also **Figure 1—figure supplements 1–4, Figure 1—source data 1, 2**.

DOI: [10.7554/eLife.02866.003](https://doi.org/10.7554/eLife.02866.003)

PDB ID(large)	Details	Amino acids
2g30_A	Chain A, Beta Appendage Of Ap2 Complexed With Arh Peptide	258
2vgl_A	Chain A, Ap2 Clathrin Adaptor Core	621
2vgl_B	Chain B, Ap2 Clathrin Adaptor Core	591
3hs8_A	Chain A, Intersectin 1-Peptide-Ap2 Alpha Ear Complex	273
2e9g_A	Chain A, Solution Structure Of The Alpha Adaptinc2 Domain From Human Adapter-Related Protein Complex 1 Gamma 2 Subunit.	131
3zy7_A	Chain A, Crystal Structure Of Computationally Redesigned Gamma-Adaptin Appendage Domain Forming A Symmetric Homodimer.	122
1iu1_A	Chain A, Crystal Structure Of Human Gamma1-Adaptin Ear Domain.	146
1kyf_A	Chain A, Ap-2 Clathrin Adaptor Alpha-Appendage In Complex With Eps15 Dpf Peptide.	247
1w63_A	Chain A, Ap1 Clathrin Adaptor Core.	618
1gyu_A	Chain A, Gamma-Adaptin Appendage Domain From Clathrin Adaptor Ap1.	140
1w63_B	Chain B, Ap1 Clathrin Adaptor Core	584
PDB ID (medium & small)	Details	Amino acids
3l81_A	Chain A, Crystal Structure Of Adaptor Protein Complex 4 (Ap-4) Mu Su Terminal Domain, In Complex With A Sorting Peptide From The Precursor Protein (App).	301
2vgl_M	Chain M, Ap2 Clathrin Adaptor Core	435
2vgl_S	Chain S, Ap2 Clathrin Adaptor Core	142
1w63_M	Chain M, Ap1 Clathrin Adaptor Core	423
1w63_Q	Chain Q, Ap1 Clathrin Adaptor Core	158
1i31_A	Chain A, Mu2 Adaptin Subunit (Ap50) Of Ap2 Clathrin Adaptor, Complexed With Egfr Internalization Peptide Fyralm	314

Figure 1—figure supplement 1. PDB entries used to search for adaptor-related proteins.

DOI: [10.7554/eLife.02866.006](https://doi.org/10.7554/eLife.02866.006)

Figure 1—figure supplement 2. Summary table of all subunits identified using reverse HHpred.
DOI: 10.7554/eLife.02866.007

	Accession	Amino acids	ID
<i>Arabidopsis thaliana</i>	NP_001189515.1	1198	TSAUCER
<i>Selaginella moellendorffii</i>	XP_002983953.1	1058	TSAUCER
<i>Selaginella moellendorffii</i>	XP_002960718.1	1058	TSAUCER
<i>Vitis vinifera</i>	XP_002275101.1	1202	TSAUCER
<i>Volvox carteri</i>	XP_002954451.1	1376	TSAUCER
<i>Micromonas pusilla</i>	XP_003058310.1	848	TSAUCER
<i>Micromonas pusilla</i>	XP_003055695.1	1529	TPLATE
<i>Physcomitrella patens</i>	XP_001755114.1	579	AP-5 ζ
<i>Physcomitrella patens</i>	XP_001753717.1	574	AP-5 ζ
<i>Arabidopsis thaliana</i>	NP_188621.2	1090	AP-5 $\beta 5$
<i>Selaginella moellendorffii</i>	XP_002960166.1	1121	AP-5 $\beta 5$
<i>Selaginella moellendorffii</i>	XP_002983970.1	1120	AP-5 $\beta 5$
<i>Physcomitrella patens</i>	XP_001753719.1	1138	AP-5 $\beta 5$
<i>Vitis vinifera</i>	XP_002272061.2	1099	AP-5 $\beta 5$
<i>Dictyostelium discoideum</i>	XP_640040.1	1398	AP-5 $\beta 5$
<i>Homo sapiens</i>	NP_612377.4	878	AP-5 $\beta 5$
<i>Naegleria gruberi</i>	XP_002677583.1	1758	AP-5 $\beta 5$
<i>Homo sapiens</i>	NP_060817	200	AP-5 $\sigma 5$
<i>Giardia lamblia</i>	XP_001704530.1	960	γ -COP
<i>Naegleria gruberi</i>	XP_002683551.1	143	ζ -COP

Figure 1—figure supplement 3. Subunits that failed to be identified using reverse HHpred, but were identified by homology searching using NCBI BLAST.

DOI: [10.7554/eLife.02866.008](https://doi.org/10.7554/eLife.02866.008)

	β -like (TPLATE)	$\alpha\gamma\delta\epsilon\zeta$ - like (TSAUCER)	μ -like (TCUP)	σ -like (TSPOON)	β' -COP like (TTRAY1)	β' -COP like (TTRAY2)
<i>Arabidopsis thaliana</i>	NP_186827.2 (TPLATE)	NP_001189515.1 (TASH3)	NP_200555.1 (TML)	NP_172989.1 (LOLITA)	NP_190628.6 (TWD40-1)	NP_197859.4 (TWD40-2)
<i>Selaginella moellendorffii</i>	XP_002985757.1 XP_002974452.1	XP_002983953.1 XP_002960718.1	XP_002983631.1	XP_002974400.1 XP_002985698.1	XP_002988683.1 XP_002986386.1	XP_002969859.1 XP_002985192.1
<i>Physcomitrella patens</i>	XP_001753083.1 XP_001764266.1 XP_001761456.1	Pp1s206_101V6.1	XP_001784609.1	XP_001752367.1	XP_001761291.1	XP_001757483.1
<i>Vitis vinifera</i>	XP_002263932.1	XP_002275101.1	XP_002271128.1	XP_002268544.1	XP_003635289.1	XP_002263744.1
<i>Volvox carteri</i>	XP_002948025.1	XP_002954451.1	XP_002958785.1	XP_002949494.1	XP_002948805.1	XP_002950796.1
<i>Naegleria gruberi</i>	XP_002675144.1	XP_002677398.1	XP_002671328.1	XP_002673133.1	none identified	XP_002676398.1
<i>Micromonas pusilla</i>	XP_003055695.1	XP_003058310.1	none identified	XP_003057871.1	XP_003064579.1	191839 PACid:273 44862
<i>Dictyostelium purpureum</i>	XP_003286721.1	XP_003291898.1	DPU0040472	XP_003287313.1	XP_003287680.1	XP_003287023.1
<i>Dictyostelium discoideum</i>	XP_639969.1	XP_640471.1	XP_629998.1	DDB_G0350235	XP_642289.1	XP_637150.1

Figure 1—figure supplement 4. TSET orthologues in different species.

DOI: [10.7554/eLife.02866.009](https://doi.org/10.7554/eLife.02866.009)

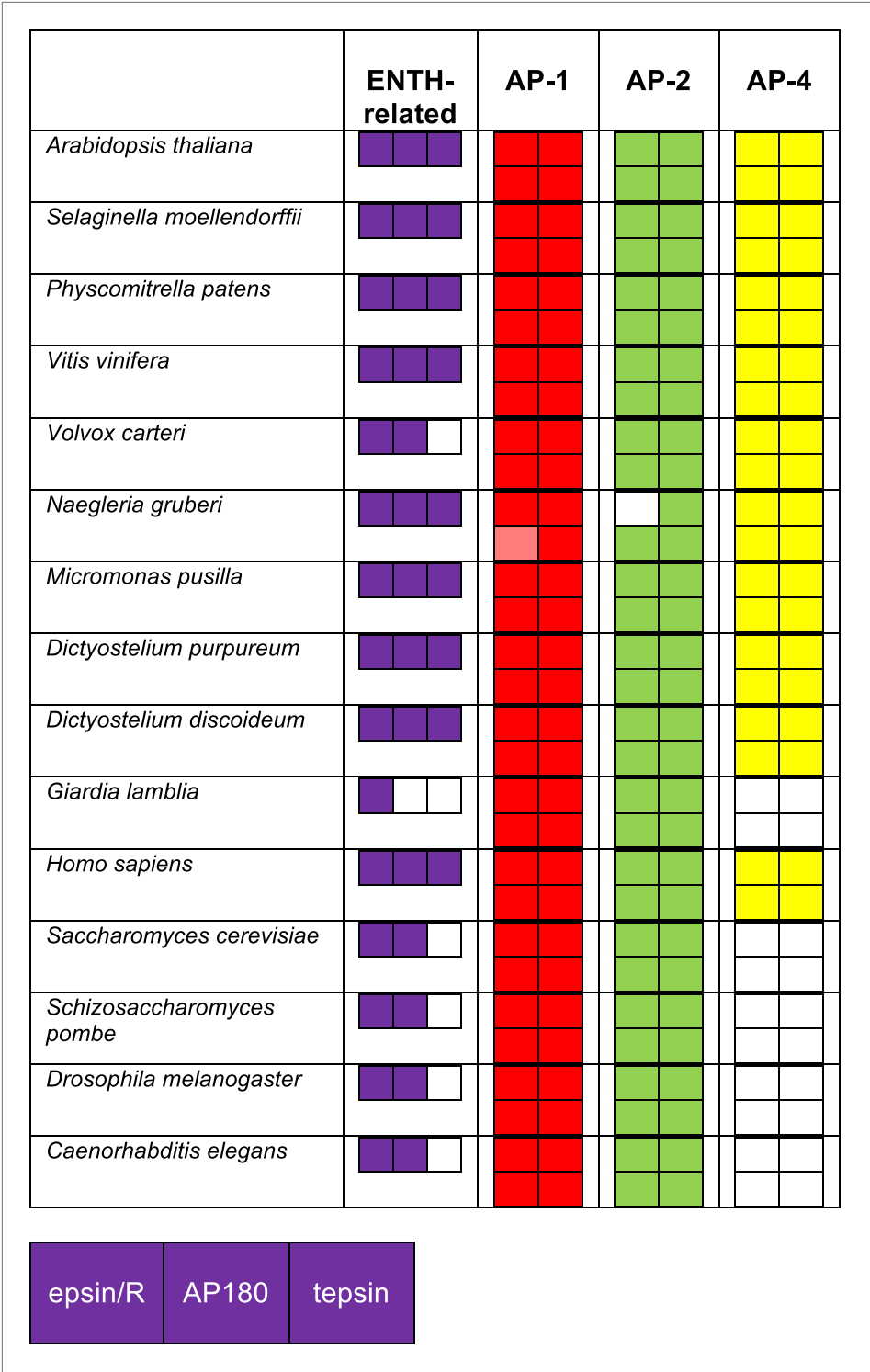


Figure 1—figure supplement 5. Identification of ENTH/ANTH domain proteins and the AP complexes with which they associate, using reverse HHpred.
DOI: 10.7554/eLife.02866.010

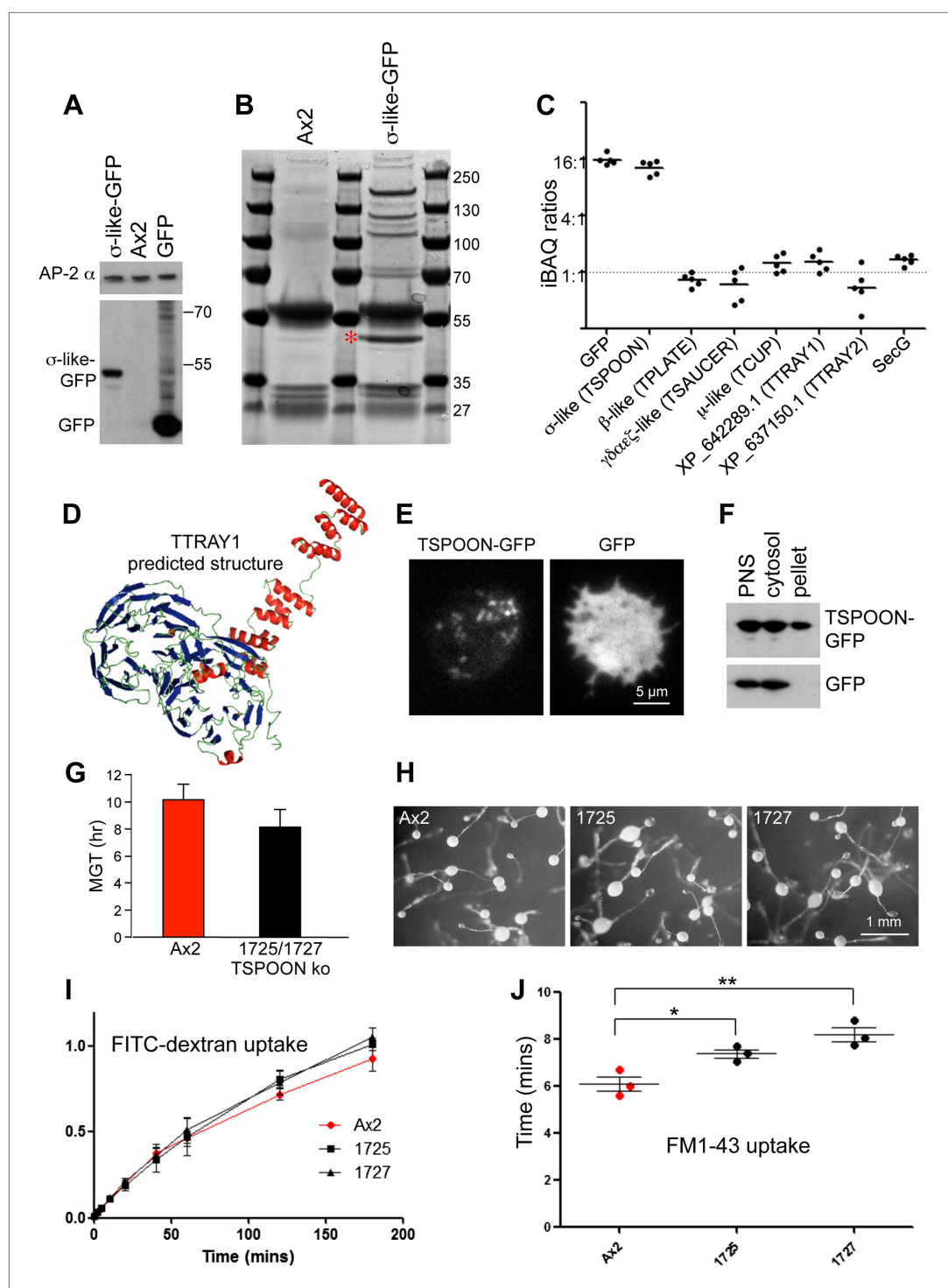


Figure 2. Characterisation of the TSET complex in *Dictyostelium*. **(A)** Western blots of axenic *D. discoideum* expressing either GFP-tagged small subunit (σ -like) or free GFP, under the control of the Actin15 promoter, labelled with anti-GFP. The Ax2 parental cell strain was included as a control, and an antibody against the AP-2 α subunit was used to demonstrate that equivalent amounts of protein were loaded. **(B)** Coomassie blue-stained gel of GFP-tagged small subunit and associated proteins immunoprecipitated with anti-GFP. The GFP-tagged protein is indicated with a red asterisk. **(C)** iBAQ ratios (an estimate of molar ratios) for the proteins that consistently coprecipitated with the GFP-tagged small subunit. All appear to be equimolar with each other, and the higher ratios for the small (σ -like/TSPOON) subunit and GFP are likely to be a consequence of their overexpression, which we also saw in a repeat. *Figure 2. Continued on next page*

Figure 2. Continued

experiment in which we used the small subunit's own promoter (**Figure 2—figure supplement 1**). **(D)** Predicted structure of the N-terminal portion of *D. discoideum* TTRAY1, shown as a ribbon diagram. **(E)** Stills from live cell imaging of cells expressing either TSPOON-GFP or free GFP, using TIRF microscopy. The punctate labelling in the TSPOON-GFP-expressing cells indicates that some of the construct is associated with the plasma membrane. See **Videos 1 and 2**. **(F)** Western blots of extracts from cells expressing either TSPOON-GFP or free GFP. The post-nuclear supernatants (PNS) were centrifuged at high speed to generate supernatant (cytosol) and pellet fractions. Equal protein loadings were probed with anti-GFP. Whereas the GFP was exclusively cytosolic, a substantial proportion of TSPOON-GFP fractionated into the membrane-containing pellet. **(G)** Mean generation time (MGT) for control (Ax2) and TSPOON knockout cells. The knockout cells grew slightly faster than the control. **(H)** Differentiation of the Ax2 control strain and two TSPOON knockout strains (1725 and 1727). All three strains produced fruiting bodies upon starvation. **(I)** Assay for fluid phase endocytosis. The control and knockout strains took up FITC-dextran at similar rates. **(J)** Assay for endocytosis of membrane, labelled with FM1-43, showing the time taken to internalise the entire surface area. The knockout strains took significantly longer than the control (* $p < 0.05$; ** $p < 0.01$). See also **Figure 2—figure supplements 1 and 2**, **Figure 2**, **Videos 1 and 2**.

DOI: [10.7554/eLife.02866.011](https://doi.org/10.7554/eLife.02866.011)



Species	Annotation	Accession
<i>Dictyostelium discoideum</i>	SecG	XP_637214.1
<i>Acanthamoeba castellanii</i>	SecG	XP_004339446
<i>Polysphondylium pallidum</i>	SecG	EFA81640

Figure 2—figure supplement 2. Distribution of secG.

DOI: [10.7554/eLife.02866.013](https://doi.org/10.7554/eLife.02866.013)

Species	Annotation	Accession
<i>Dictyostelium discoideum</i>	Vacuolin A	XP_636194.1
	Vacuolin B	XP_641785.1
	Vacuolin C	XP_641784.1
<i>Acanthamoeba castellanii</i>	Vacuolin B	XP_004344121.1
	Vacuolin B	XP_004344100.1
<i>Polysphondylium pallidum</i>	Vacuolin A	EFA84974.1
	Vacuolin A	EFA82673.1
	Vacuolin A	EFA82573.1
	Vacuolin A	EFA78749.1
<i>Bigelowiella natans</i>	Vacuolin B	jgi Bigna1 86747 estExt_fgenes1_pg.C_130159
	Vacuolin B	jgi Bigna1 131962 aug1.16_g6670
	Vacuolin B	jgi Bigna1 85415 estExt_fgenes1_pg.C_40040
	Vacuolin B	jgi Bigna1 64640 fgenes1_kg.81_#_12_#_4008_1_CFAO_EXT
<i>Bodo saltans</i>	Vacuolin A	BS69240
	Vacuolin C	BS63415
	Vacuolin C	BS79800
<i>Naegleria gruberi</i>	Vacuolin A	jgi Naegr1 78343 estExt_fgenesNG_pg.C_50301
	Vacuolin A	jgi Naegr1 81131 estExt_fgenesNG_pg.C_510098
<i>Thecamonas trahens</i>	Vacuolin A	AMSG_01405T0
<i>Chlamydomonas reinhardtii</i>	Vacuolin A	Cre06.g299550.t1.2
<i>Dictyostelium purpureum</i>	Vacuolin A	XP_003287744.1
	Vacuolin A	XP_003284594.1
<i>Micromonas pusill</i>	Vacuolin A	56078 PACid:27347119
<i>Trichomonas vaginalis</i>	Vacuolin C	TVAG_115310
	Vacuolin A	TVAG_460920
	Vacuolin A	TVAG_302990
<i>Tetrahymena thermophila</i>	Vacuolin A	3729.m00027
	Vacuolin B	3729.m00022
	VacuolinB	3729.m00026

Figure 2—figure supplement 3. Distribution of vacuolins.

DOI: [10.7554/eLife.02866.014](https://doi.org/10.7554/eLife.02866.014)

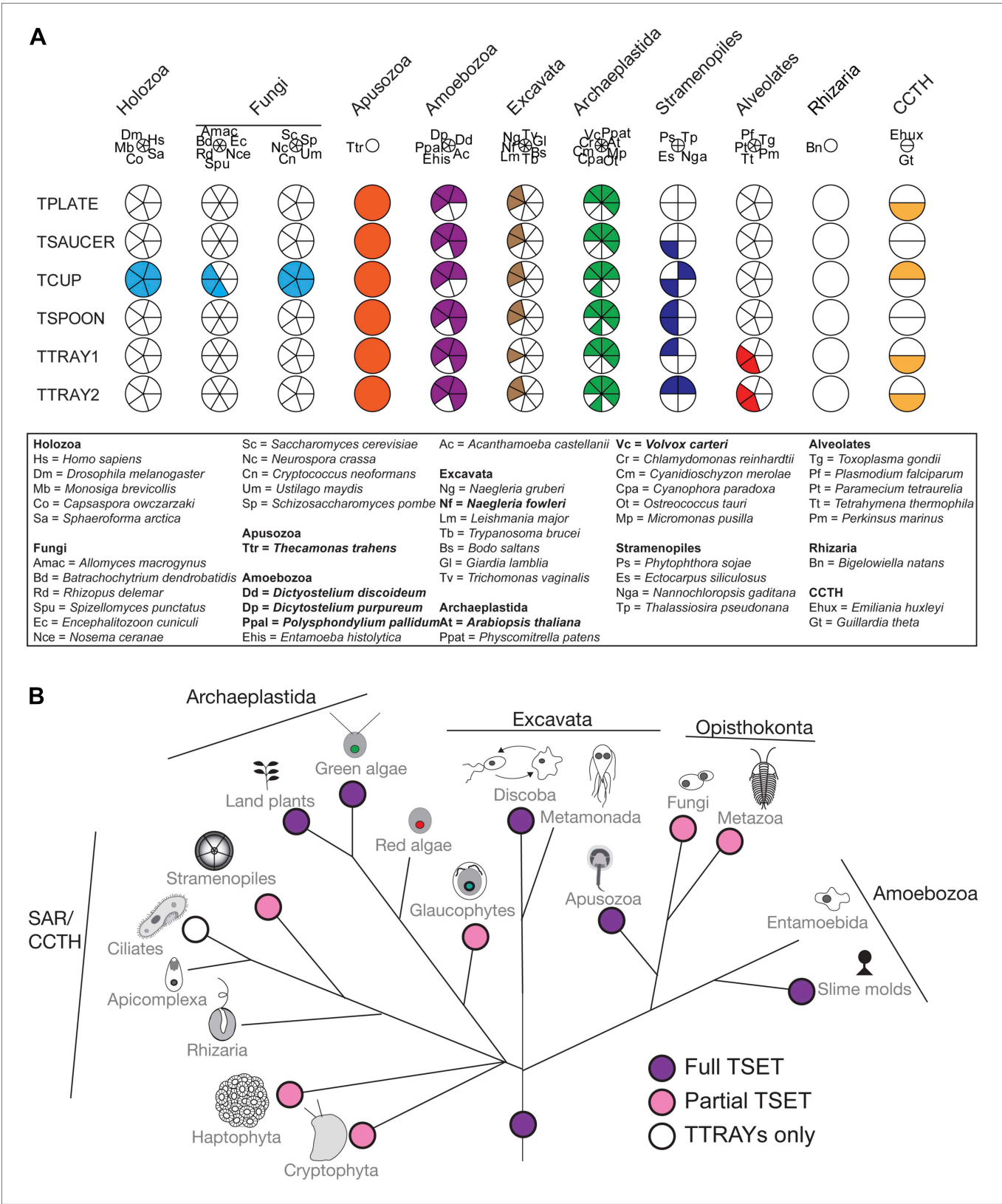


Figure 3. Distribution of TSET subunits. **(A)** Coulson plot showing the distribution of TSET in a diverse set of representative eukaryotes. Presence of the entire complex in at least four supergroups suggests its presence in the last eukaryotic common ancestor (LECA) with frequent secondary loss. Solid sectors indicate sequences identified and classified using BLAST and HMMer. Empty sectors indicate taxa in which no significant orthologues were identified. **(B)** Phylogenetic tree showing the distribution of TSET subunits across various eukaryotic supergroups. The tree is rooted at the base and branches out to show the relationships between different groups. The groups are color-coded: purple for Full TSET, pink for Partial TSET, and white for TTRAYs only. The groups include Archaeplastida, Excavata, Opisthokonta, SAR/CCTH, and Amoebozoa. The SAR/CCTH group includes Green algae, Land plants, Red algae, Glaucophytes, Stramenopiles, Ciliates, Apicomplexa, Rhizaria, Haptophyta, and Cryptophyta. The Excavata group includes Discoba, Metamonada, and Apusozoa. The Opisthokonta group includes Fungi, Metazoa, and Amoebozoa. The Amoebozoa group includes Entamoebida and Slime molds.

Figure 3. Continued

identified. Filled sectors in the Holozoa and Fungi represent F-BAR domain-containing FCHo and Syp1, respectively. Taxon name abbreviations are inset. Names in bold indicate taxa with all six components. **(B)** Deduced evolutionary history of TSET as present in the LECA but independently lost multiple times, either partially or completely. See also **Figure 3—source data 1**, **Figure 3—figure supplement 1**.

DOI: [10.7554/eLife.02866.017](https://doi.org/10.7554/eLife.02866.017)

Figure	Dataset	Method	Model	Number of characters	Number of Taxa
Concatenation	Concat.R6	MrBayes	mixed + gamma	1466	112
		PhyloBayes	LG+CAT	1466	112
		PhyML	LG+I+G+F	1466	112
		RAxML	LG+CAT+F	1466	112
TPLATE_WC	TPLATE.R2	MrBayes	mixed + gamma	560	121
		RAxML	LG+CAT+F	560	121
TPLATE_WOC	TPLATE.R4	MrBayes	mixed + gamma	402	91
		RAxML	LG+CAT+F	402	91
TSAUCER_WC	TSAUCER.R2	MrBayes	mixed + gamma	562	154
		RAxML	LG+CAT+F	562	154
TSAUCER_WOC	TSAUCER.R4	MrBayes	mixed + gamma	284	123
		RAxML	LG+CAT+F	284	123
TCUP_WC	TCUP.R2	MrBayes	mixed + gamma	379	159
		RAxML	LG+CAT+F	379	159
TCUP_WOC	TCUP.R4	MrBayes	mixed + gamma	187	133
		RAxML	LG+CAT+F	187	133
TSPOON_WC	TSPOON.R2	MrBayes	mixed + gamma	141	139
		RAxML	LG+CAT+F	141	139
TTRAY	TTRAY.R4	MrBayes	mixed + gamma	437	60
		RAxML	LG+CAT+F	437	60

Figure 3—figure supplement 1. Models used for phylogenetic analyses.

DOI: [10.7554/eLife.02866.019](https://doi.org/10.7554/eLife.02866.019)

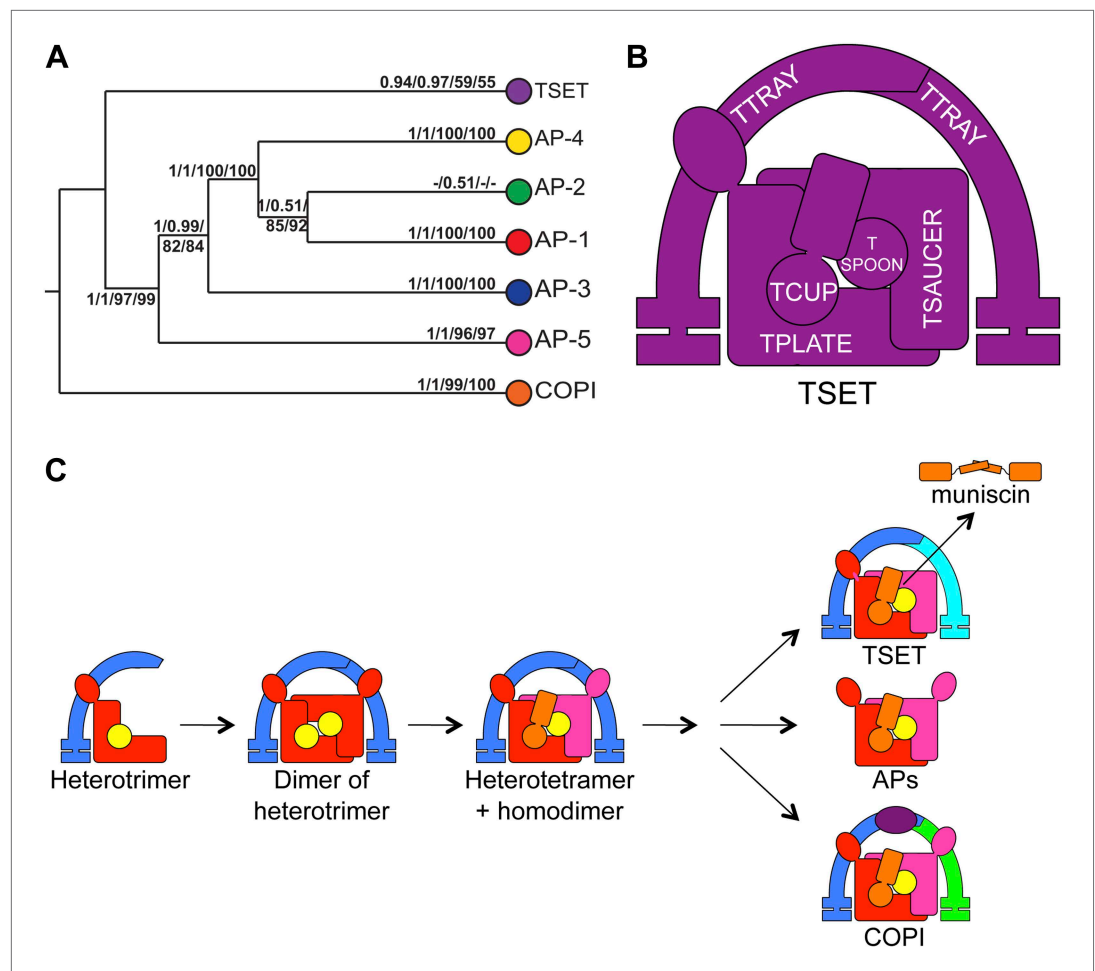


Figure 4. Evolution of TSET. **(A)** Simplified diagram of the concatenated tree for TSET, APs, and COPI, based on **Figure 4—figure supplement 8**. Numbers indicate posterior probabilities for MrBayes and PhyloBayes and maximum-likelihood bootstrap values for PhyML and RAxML, in that order. **(B)** Schematic diagram of TSET. **(C)** Possible evolution of the three families of heterotetramers: TSET, APs, and COPI. We propose that the earliest ancestral complex was a likely a heterotrimer or a heterohexamer formed from two identical heterotrimers, containing large (red), small (yellow), and scaffolding (blue) subunits. All three of these proteins were composed of known ancient building blocks of the membrane-trafficking system (Vedovato et al., 2009): α -solenoid domains in both the large and scaffolding subunits; two β -propellers in the scaffolding subunit; and a longin domain forming the small subunit. The gene encoding the large subunit then duplicated and mutated to generate the two distinct types of large subunits (red and magenta), and the gene encoding the small subunit also duplicated and mutated (yellow and orange), with one of the two proteins (orange) acquiring a μ homology domain (MHD) to form the ancestral heterotetramer, as proposed by Boehm and Bonifacio (12). However, the scaffolding subunit remained a homodimer. Upon diversification into three separate families, the scaffolding subunit duplicated independently in TSET and COPI, giving rise to TTRAY1 and TTRAY2 in TSET, and to α - and β -COP in COPI. COPI also acquired a new subunit, ϵ -COP (purple). The scaffolding subunit may have been lost in the ancestral AP complex, as indicated in the diagram; however, AP-5 is tightly associated with two other proteins, SPG11 and SPG15, and the relationship of SPG11 and SPG15 to TTRAY/B-COP remains unresolved, so it is possible that SPG11 and SPG15 are highly divergent descendants of the original scaffolding subunits. The other AP complexes are free heterotetramers when in the cytosol, but membrane-associated AP-1 and AP-2 interact with another scaffold, clathrin; and AP-3 has also been proposed to interact transiently with a protein with similar architecture, Vps41 (Rehling et al., 1999; Cabrera et al., 2010; Asensio et al., 2013). So far no scaffold has been proposed for AP-4. Although the order of emergence of TSET and COP relative to adaptins is unresolved, our most recent analyses indicate that, contrary to previous reports (Hirst et al., 2011), AP-5 diverged basally within the adaptin clade, followed by AP-3, AP-4, and APs 1 and 2, all prior to the LECA. This still suggests a primordial bridging of the secretory and phagocytic systems prior to emergence of a *trans*-Golgi Figure 4. Continued on next page

Figure 4. Continued

network. The muniscins arose much later, in ancestral opisthokonts, from a translocation of the TSET MHD-encoding sequence to a position immediately downstream from an F-BAR domain-encoding sequence. Another translocation occurred in plants, where an SH3 domain-coding sequence was inserted at the 3' end of the TSAUCER-coding sequence. See also **Figure 4—figure supplements 1–10**.

DOI: [10.7554/eLife.02866.020](https://doi.org/10.7554/eLife.02866.020)

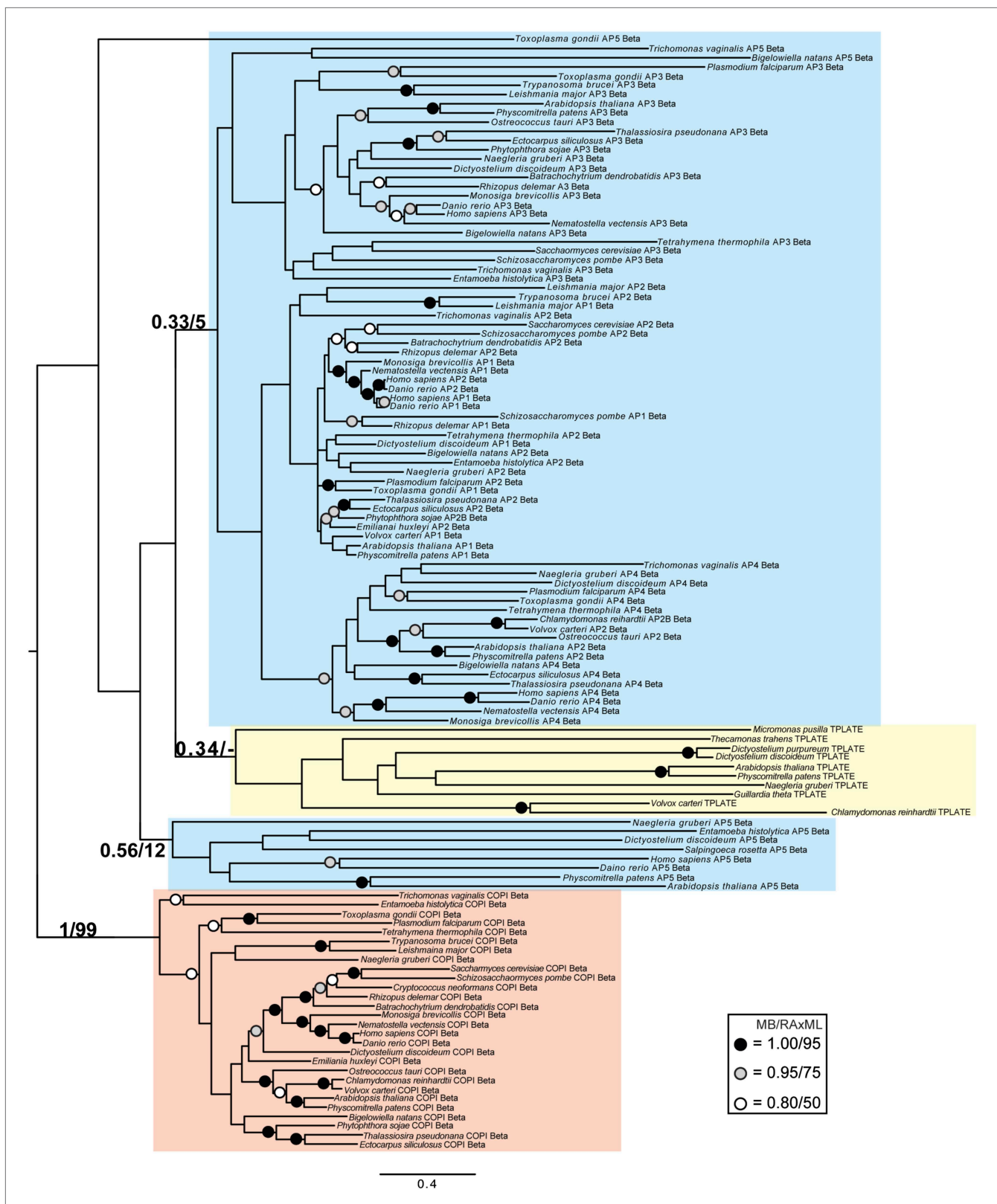


Figure 4—figure supplement 1. Phylogenetic analysis of TPLATE, β -COP, and β -adaptin, with TPLATE robustly excluded from the β -COP clade.

DOI: 10.7554/eLife.02866.021

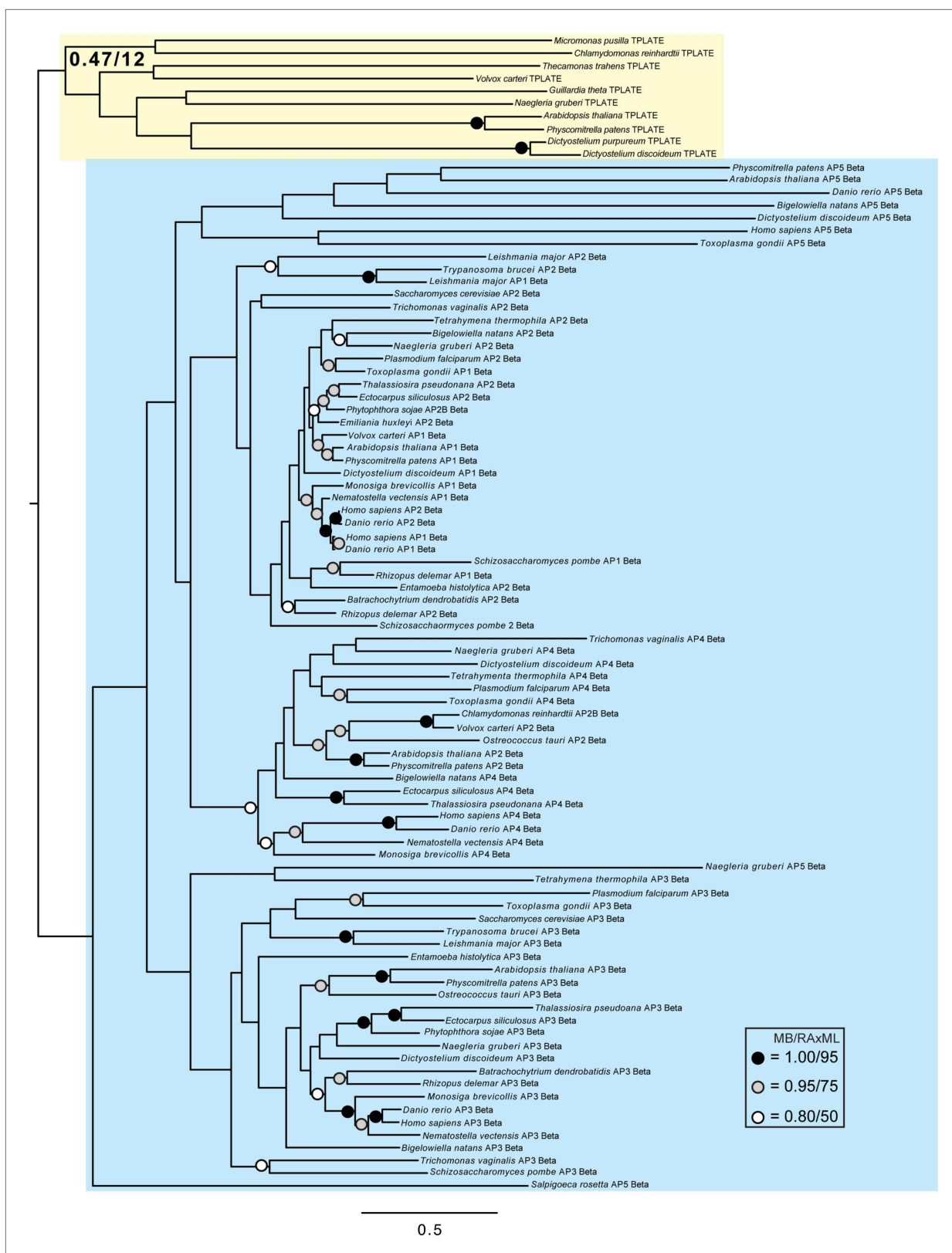


Figure 4—figure supplement 2. Phylogenetic analysis of TPLATE and β -adaptin subunits (β -COP removed) showing, with weak support, that TPLATE is excluded from the adaptin clade.

DOI: [10.7554/eLife.02866.022](https://doi.org/10.7554/eLife.02866.022)



Figure 4—figure supplement 3. Phylogenetic analysis of TSAUCER, γ -COP, and $\gamma\delta\epsilon\zeta$ -adaptin subunits, with TCUP robustly excluded from the γ -COP clade, and weakly excluded from the adaptin clade.

DOI: [10.7554/eLife.02866.023](https://doi.org/10.7554/eLife.02866.023)

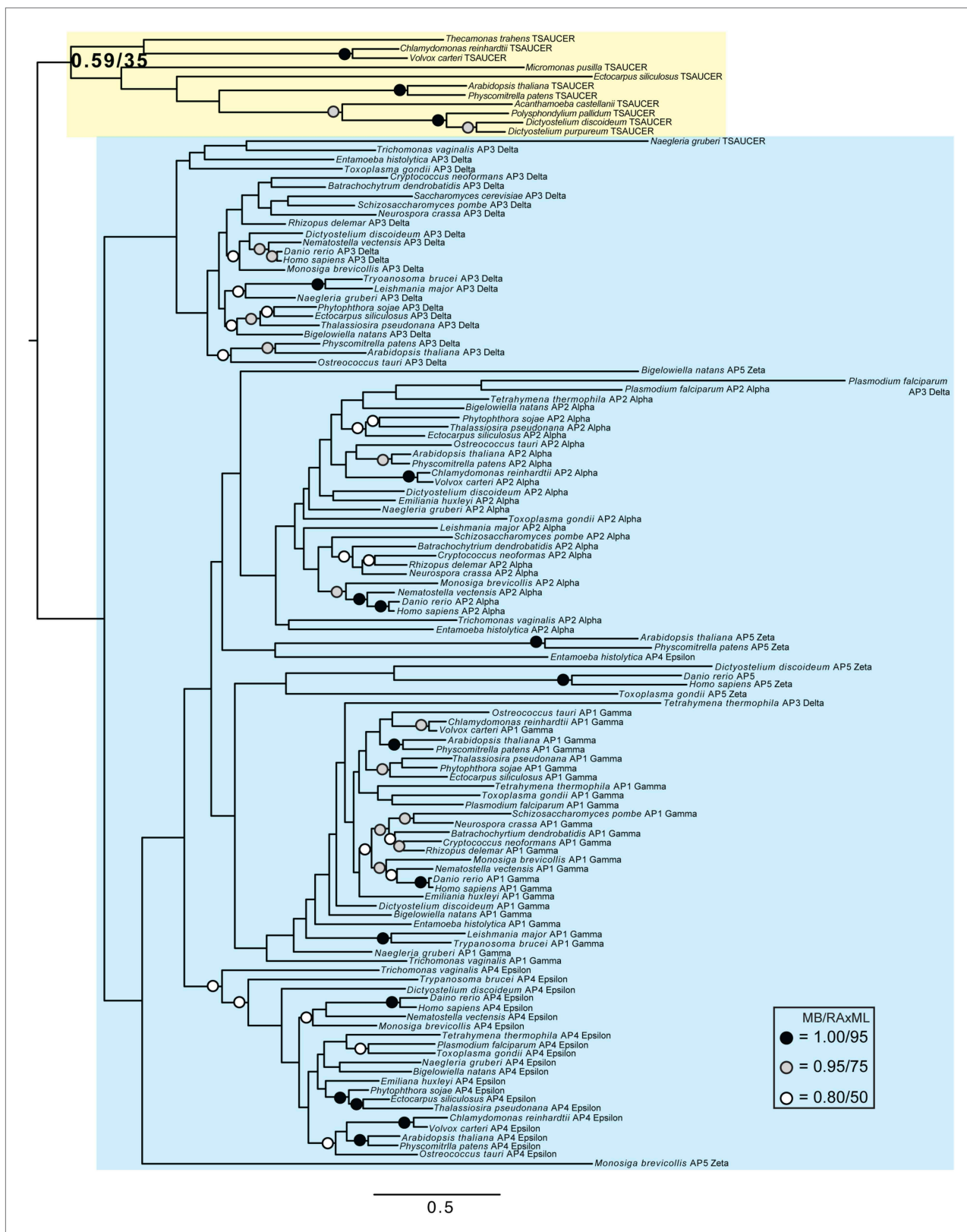


Figure 4—figure supplement 4. Phylogenetic analysis of TSAUCER and $\gamma\alpha\delta\epsilon\zeta$ -adaptin subunits (γ -COP removed), showing weak support for the exclusion of TSAUCER from the adaptin clade.

DOI: [10.7554/eLife.02866.024](https://doi.org/10.7554/eLife.02866.024)

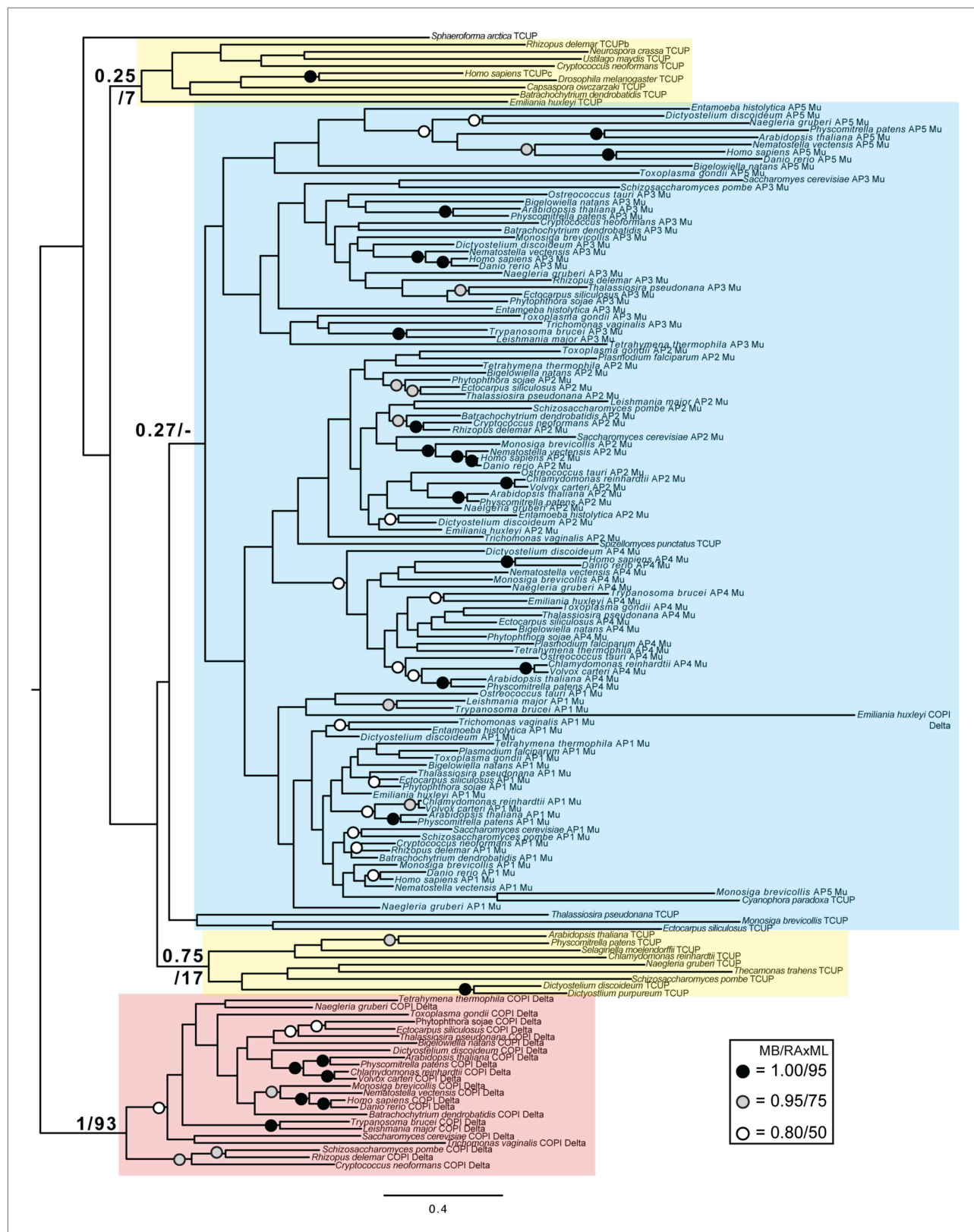


Figure 4—figure supplement 5. Phylogenetic analysis of TCUP, δ -COP, and μ -adaptin subunits, with TSAUCER robustly excluded from the δ -COP clade and weakly excluded from the adaptin clade.

DOI: 10.7554/eLife.02866.025

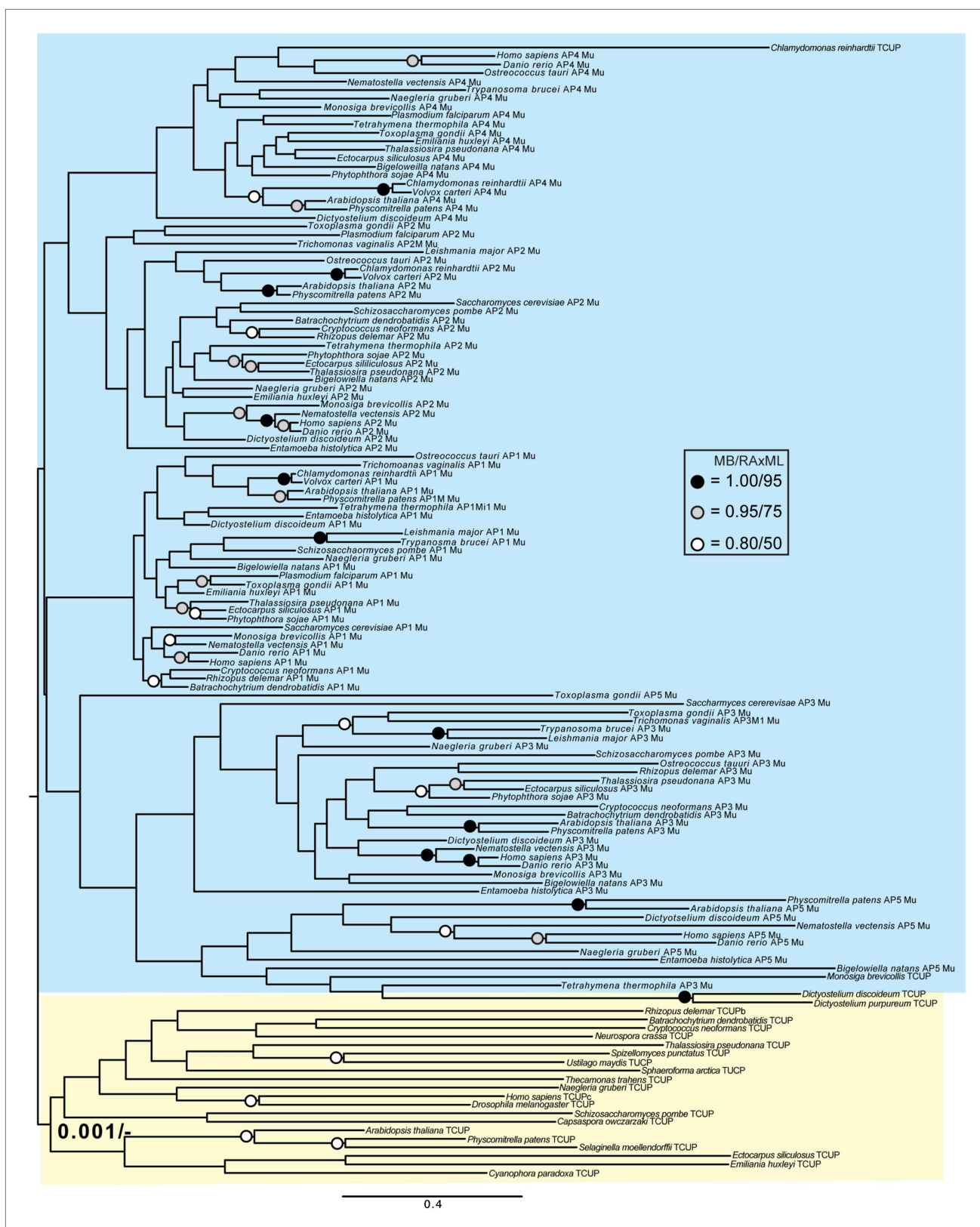


Figure 4—figure supplement 6. Phylogenetic analysis of TCUP and μ -adaplin subunits (δ -COP removed), showing weak support for the exclusion of TCUP from the adaplin clade.

DOI: [10.7554/eLife.02866.026](https://doi.org/10.7554/eLife.02866.026)

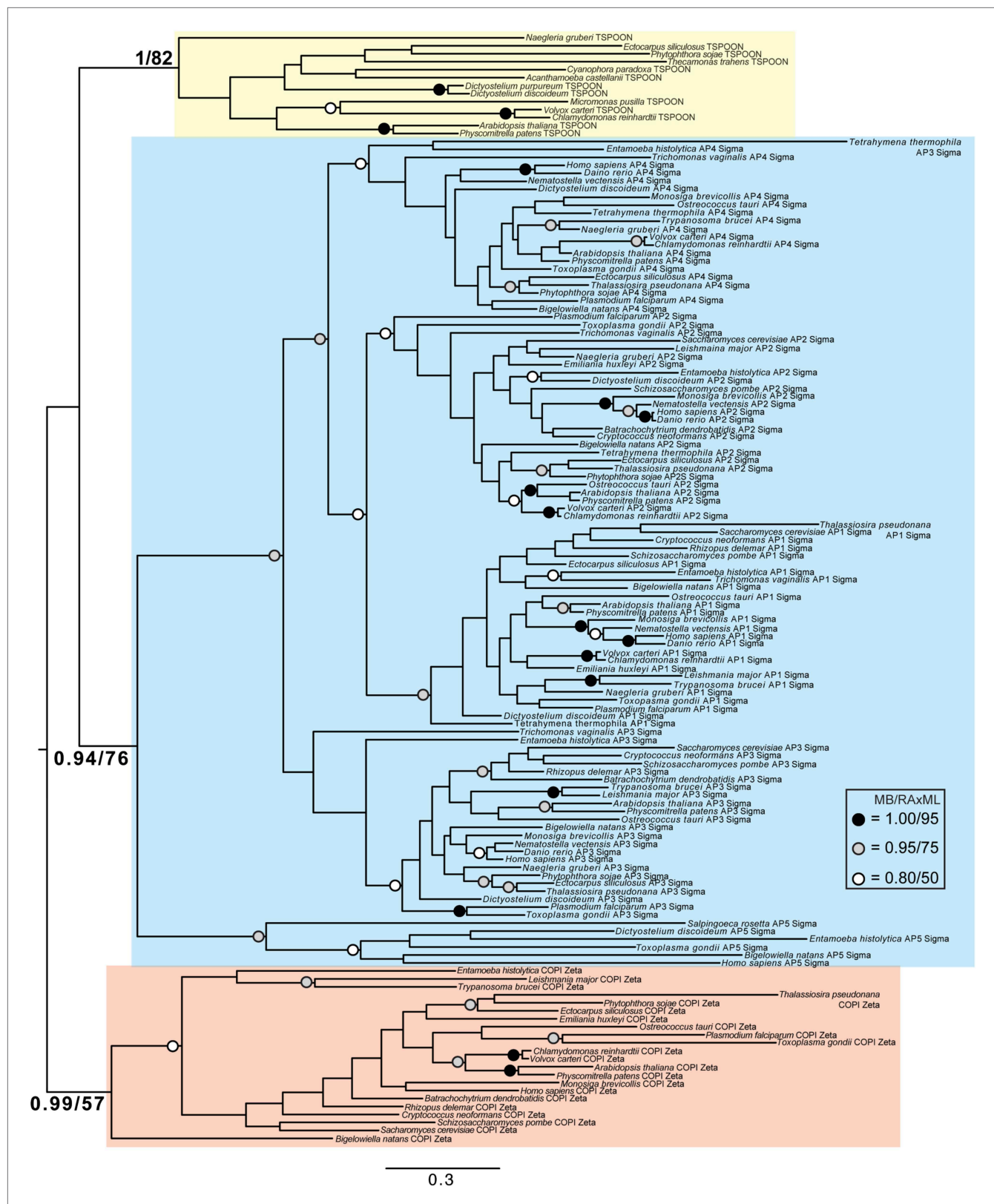


Figure 4—figure supplement 7. Phylogenetic analysis of TSPOON with ζ -COP and σ -adaptin subunits with moderate support for the exclusion of TSPOON from both the COP1 and adaptin clades, in addition to moderate support for the monophyly of the TSPOON clade.

DOI: [10.7554/eLife.02866.027](https://doi.org/10.7554/eLife.02866.027)

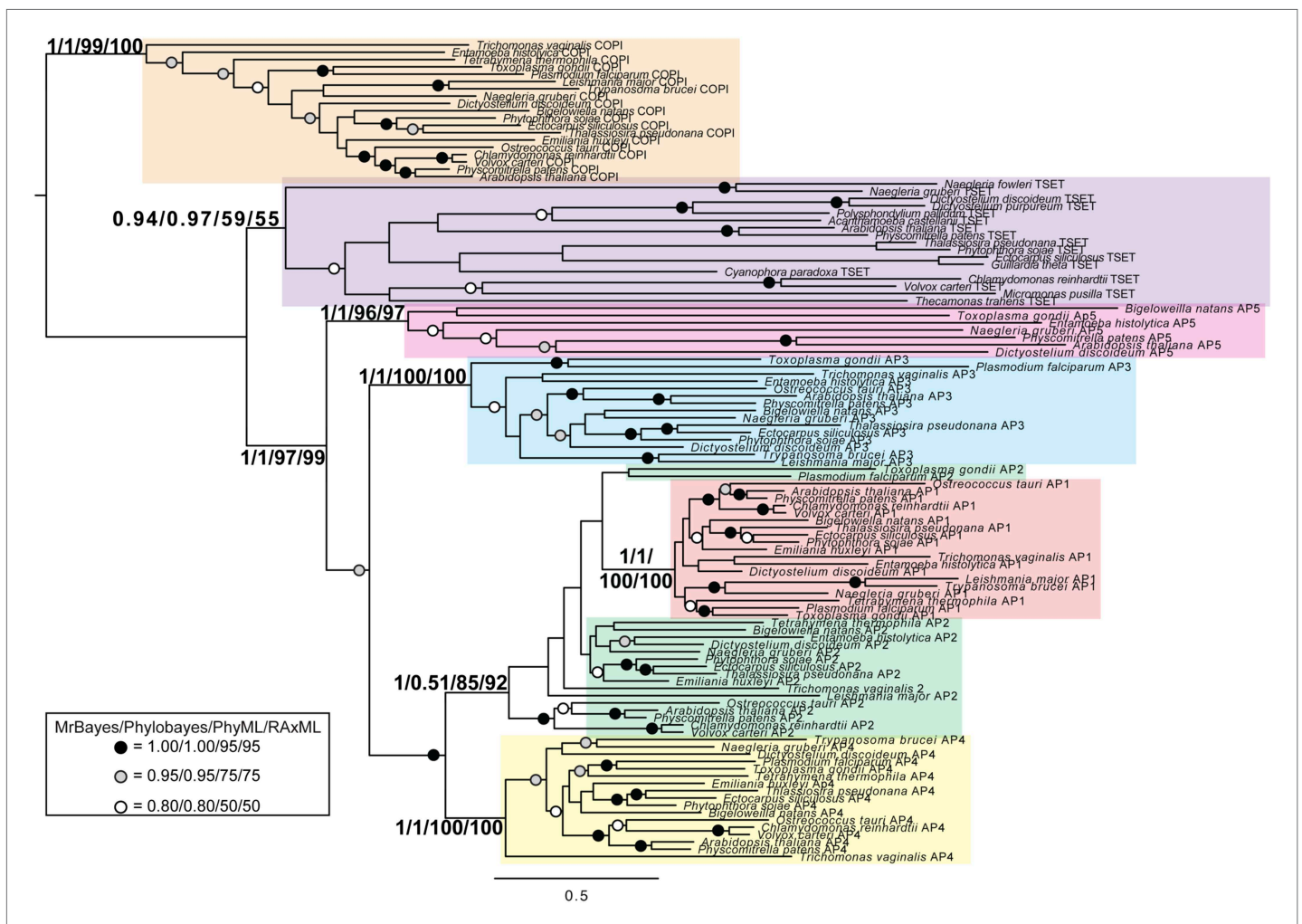


Figure 4—figure supplement 8. TSET is a phylogenetically distinct lineage from F-COPI and the AP complexes.

DOI: [10.7554/eLife.02866.028](https://doi.org/10.7554/eLife.02866.028)



Figure 4—figure supplement 9. Phylogenetic analysis of TTRAY1, TTRAY2, α -COP, and β' -COP.

DOI: [10.7554/eLife.02866.029](https://doi.org/10.7554/eLife.02866.029)

<i>Homo sapiens</i>	NP_001139504.1 (FCHO2) NP_001154829.1 (FCHO1) NP_001154830.1 (FCHO1) NP_055937.1 (FCHO1) NP_620137.2 (FCHO2) NP_001154831.1 (FCHO1) NP_115667.2 (SGIP1)
<i>Saccharomyces cerevisiae</i>	NP_009959.2 (Syp1p)
<i>Schizosaccharomyces pombe</i>	NP_596299.1 (Syp1)
<i>Drosophila melanogaster</i>	NP_001097723.1 (CG8176) NP_001097724.1 (CG8176) NP_788612.1 (CG8176) NP_788613.1 (CG8176)
<i>Caenorhabditis elegans</i>	NP_493947.1 (hypothetical protein F56D12.6) NP_493948.1 (hypothetical protein F56D12.6)

Figure 4—figure supplement 10. Muniscin family members identified by reverse HHpred, using the following PDB structures.

DOI: [10.7554/eLife.02866.030](https://doi.org/10.7554/eLife.02866.030)